Cu(II)-Mediated Tautomerization for the Pyrazole-Nitrile Coupling Reaction

Chang-Chih Hsieh,[b] Chia-Wei Chen,[a] Ming-Hsi Chiang,[b,c] and Yih-Chern Horng[a]*

[a] Department of Chemistry, National Changhua University of Education, Changhua 50058, Taiwan

[b] Institute of Chemistry, Academia Sinica, Taipei 11528, Taiwan

[c] Department of Medicinal and Applied Chemistry, Kaohsiung Medical University, Kaohsiung 80708, Taiwan

* Email: ychorng@cc.ncue.edu.tw

Electronic Supporting Information

Table of Contents

Supplementary Tables and Figures

Figure S1. The time-dependent UV-vis spectra of a 4-fold excess of 3-ClPzH reacted with Cu(ClO$_4$)$_2\cdot$6H$_2$O in MeCN at 298 K.

Figure S2. The time-dependent UV-vis spectra of a 4-fold excess of 3-MePzH reacted with Cu(ClO$_4$)$_2\cdot$6H$_2$O in MeCN at 298 K.

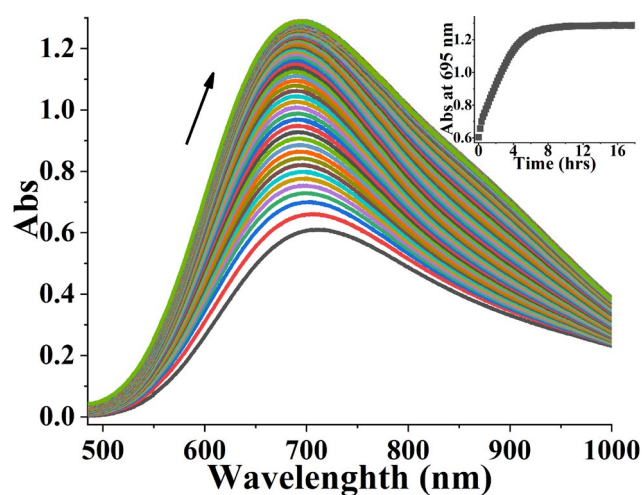**Figure S3.** The time-dependent UV-vis spectra of a 4-fold excess of 3-(t-Bu)PzH reacted with Cu(ClO$_4$)$_2\cdot$6H$_2$O in MeCN at 298 K.

Figure S4. The time-dependent UV-vis spectra of a 4-fold excess of 4-ClPzH reacted with $Cu(ClO_4)_2 \cdot 6H_2O$ in MeCN at 298 K.
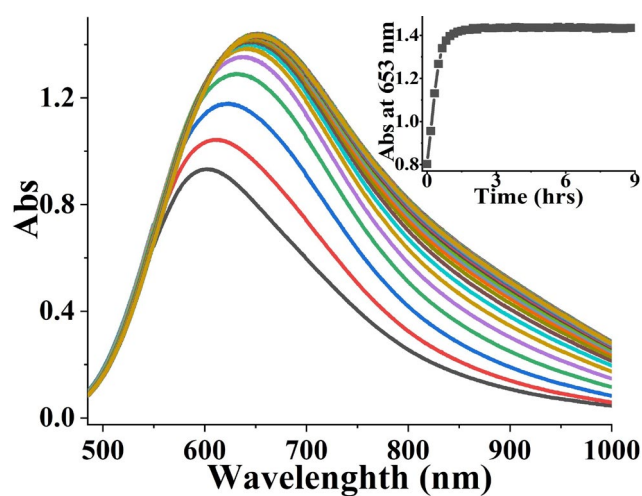
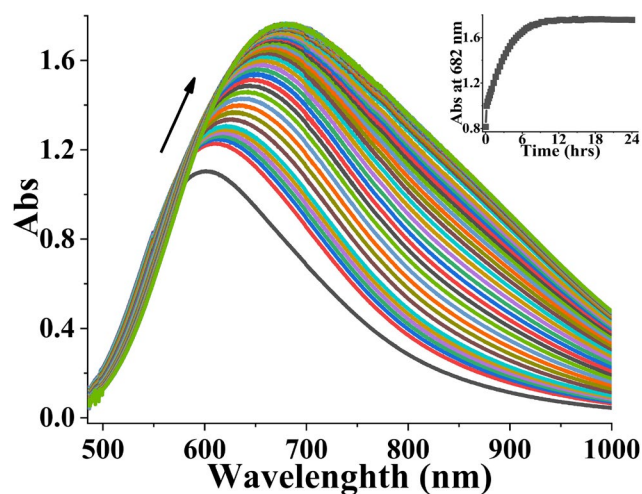**Figure S5.** The time-dependent UV-vis spectra of a 4-fold excess of 4-MePzH reacted with $Cu(ClO_4)_2 \cdot 6H_2O$ in MeCN at 298 K.
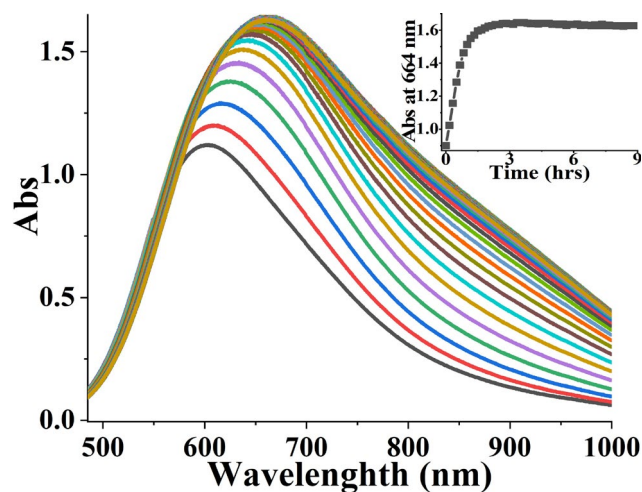
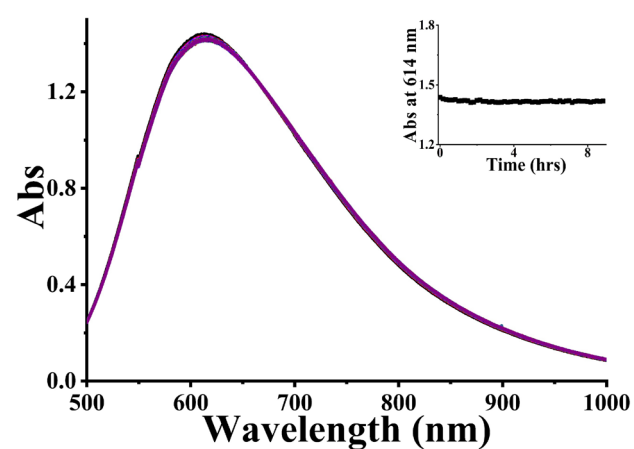**Figure S6.** The time-dependent UV-vis spectra of a 4-fold excess of 4-(t-Bu)PzH reacted with $Cu(ClO_4)_2 \cdot 6H_2O$ in MeCN at 298 K.

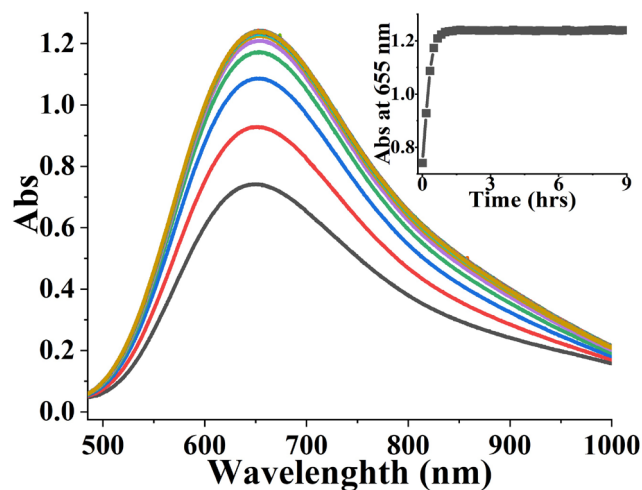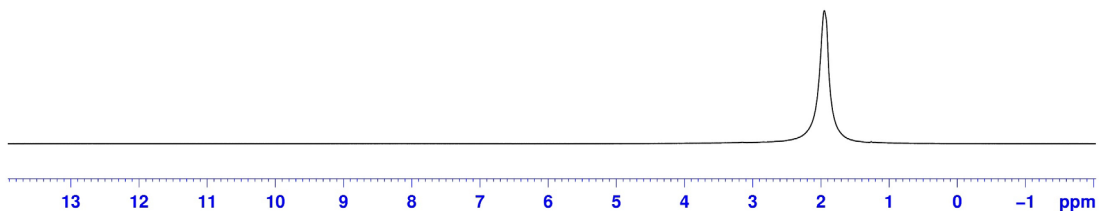**Figure S7.** ^{1}H NMR spectrum of a 4-fold excess 3-(t-Bu)PzH reacted with Cu(ClO$_4$)$_2$·6H$_2$O in d-MeCN.

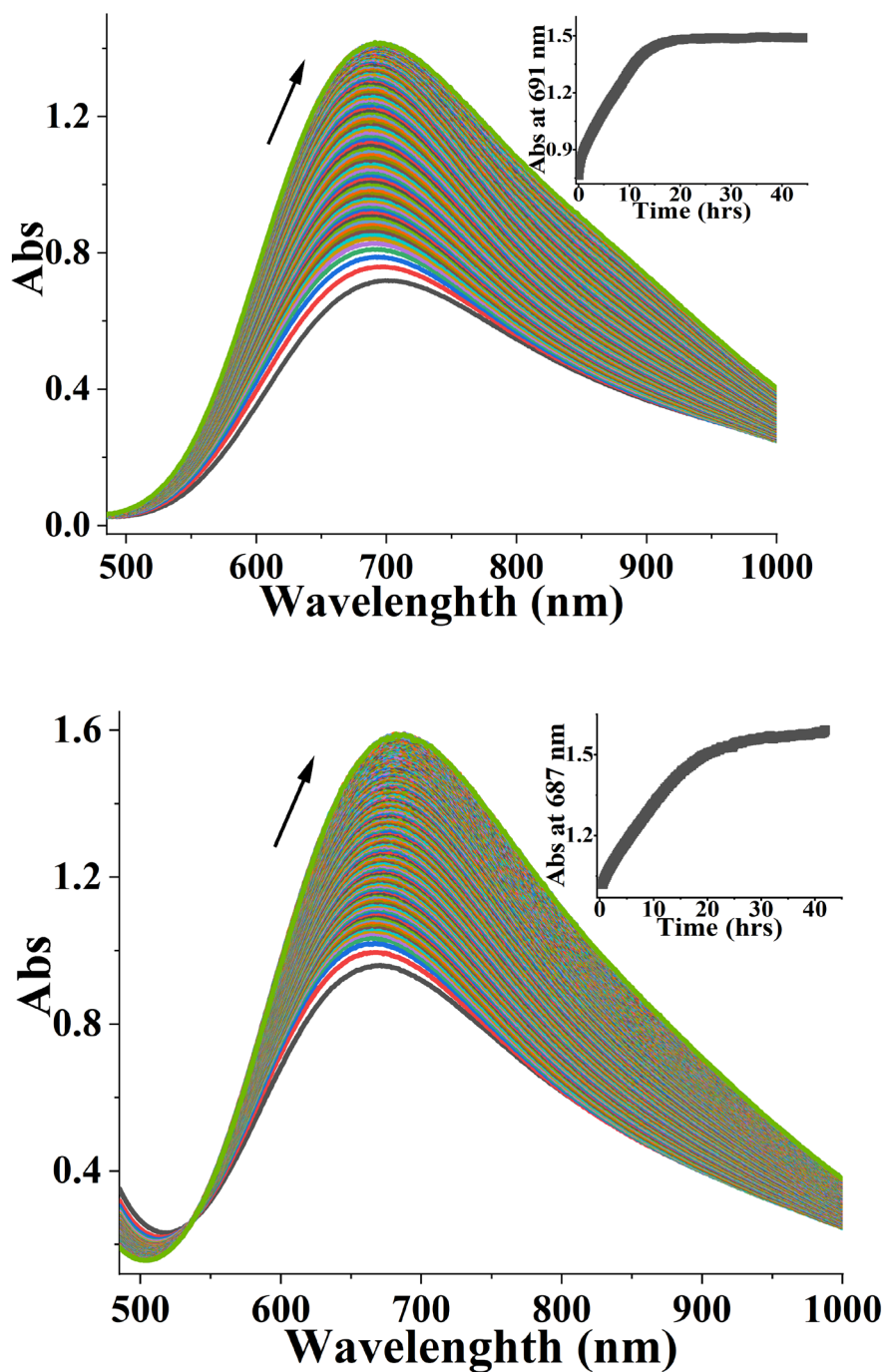**Figure S8.** The time-dependent UV-vis spectra of a 4-fold excess of 3-BrPzH (top) or 3-IPzH (bottom) reacted with Cu(ClO$_4$)$_2$·6H$_2$O in MeCN at 298 K.

Figure S9. ORTEP style representation of **1b**. Thermal ellipsoids are drawn at the 35% probability level. The hydrogen atoms bound to carbon atoms were omitted for clarity. Selected bond lengths [Å] and angles [°]: Cu1-N1 2.016(3), Cu1-N3 1.974(3), Cu1-O1 2.468(3), N1-Cu1-N3 79.37(11), N1-Cu1-O1 93.05(11), N1-Cu1-N1A 180.0, N1-Cu1-N3A 100.63(11), N1-Cu1-O1A 86.95(11), N3-Cu1-O1 84.96(12), N3-Cu1-N3A 180.0(5), N3-Cu1-O1A 95.04(12). Symmetry transformations used to generate equivalent atoms: A -x+1, -y+1, -z+1.

Figure S10. ORTEP style representation of **1c**. Thermal ellipsoids are drawn at the 35% probability level. The hydrogen atoms bound to carbon atoms were omitted for clarity. Selected bond lengths [Å] and angles [°]: Cu1-N1 2.043(4), Cu1-N3 1.975(5), Cu1-O1 2.461(4), Cu1-N1-N3 79.17(18), N1-Cu1-O1 88.75(15), N1-Cu1-N1A 180.0, N1-Cu1-N3A 100.83(18), N1-Cu1-O1A 91.25(15), N3-Cu1-O1 93.63(18), N3-Cu1-N3A 180.0, N3-Cu1-O1A 86.37(18). Symmetry transformations used to generate equivalent atoms: A -x+1, -y+1, -z+1.
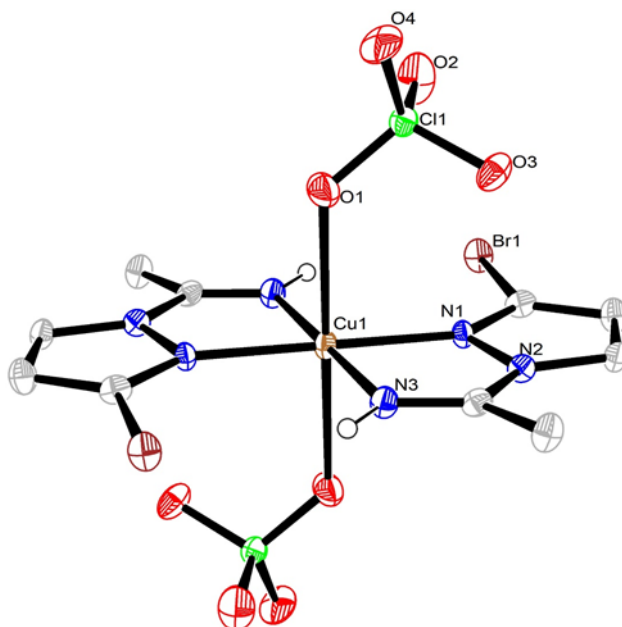
(a)

(b)

Figure S11. (a) ORTEP style representation of **1a'**. Thermal ellipsoids are drawn at the 35% probability level. The hydrogen atoms bound to carbon atoms were omitted for clarity. Selected bond lengths [Å] and angles [°]: Cu1-N1 1.9762(19), Cu1-N3 1.9688(19), Cu1-O1 2.6123(17), N1-Cu1-N3 80.36(8), N1-Cu1-O1 86.51(7), N1-Cu1-N1A 180.0, N1-Cu1-N3A 99.64(8), N1-Cu1-O1A 93.49(7), N3-Cu1-O1 90.39(7), N3-Cu1-N3A 180.0, N3-Cu1-O1A 89.61(7). Symmetry transformations used to generate equivalent atoms: A -x+1, -y+1, -z. (b) One-dimensional packing diagram with the black dashed lines showing the intermolecular NH···O hydrogen-bond interactions. Only the significant component is shown. H-bonding: N3···O2B 2.925(3) Å, H3···O2B 2.079 (2) Å, N3-H3···O2B 167.6(1)°. Symmetry code: B 1+x, y, z.
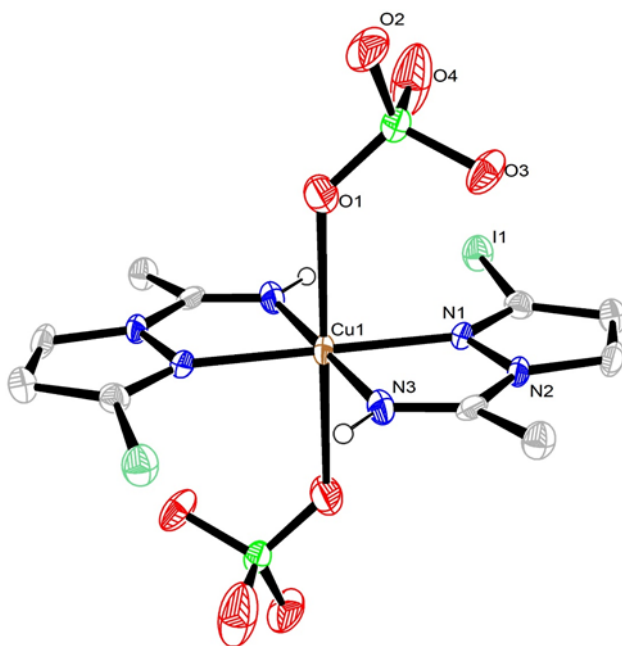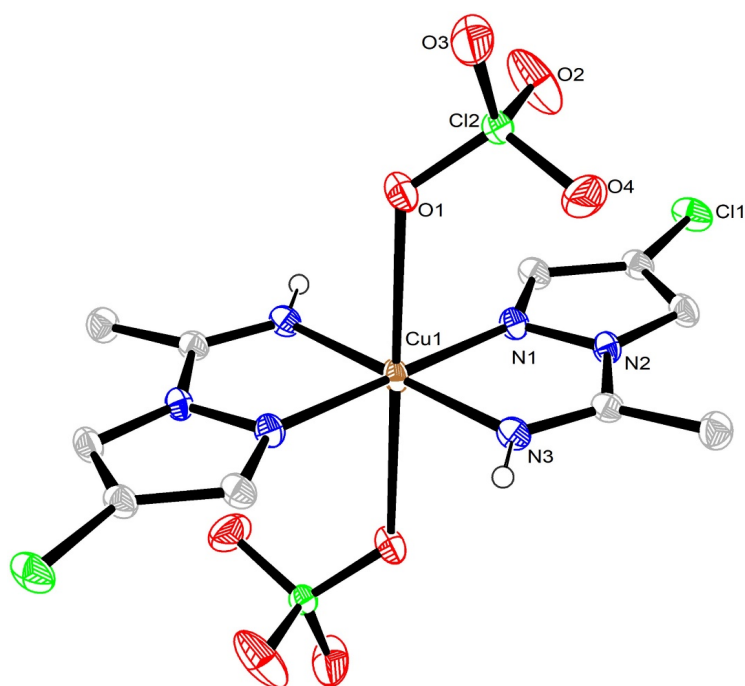
(a)

(b)

Figure S12. (a) ORTEP style representation of **1d'**. Thermal ellipsoids are drawn at the 35% probability level. The hydrogen atoms bound to carbon atoms were omitted for clarity. Selected bond lengths [Å] and angles [°]: Cu1-N1 1.980(2), Cu1-N3 1.962(2), Cu1-O1 2.532(2), N1-Cu1-N3 80.39(10), N1-Cu1-O1 89.20(9), N1-Cu1-N1A 180.00(4), N1-Cu1-N3A 99.61(10), N1-Cu1-O1A 90.80(9), N3-Cu1-O1 87.16(9), N3-Cu1-N1A 99.61(10), N3-Cu1-N3A 180.00(10), N3-Cu1-O1A 92.85(9). Symmetry transformations used to generate equivalent atoms: A -x, -y+2, -z. (b) One-dimensional packing diagram with the black dashed lines showing the intermolecular NH···O hydrogen-bond interactions. Only the significant component is shown. H-bonding: N3···O1B 2.904(4) Å, H3···O1B 2.063(3) Å, N3-H3···O1B 159.9(2)°. Symmetry code: B -1+x, y, z.
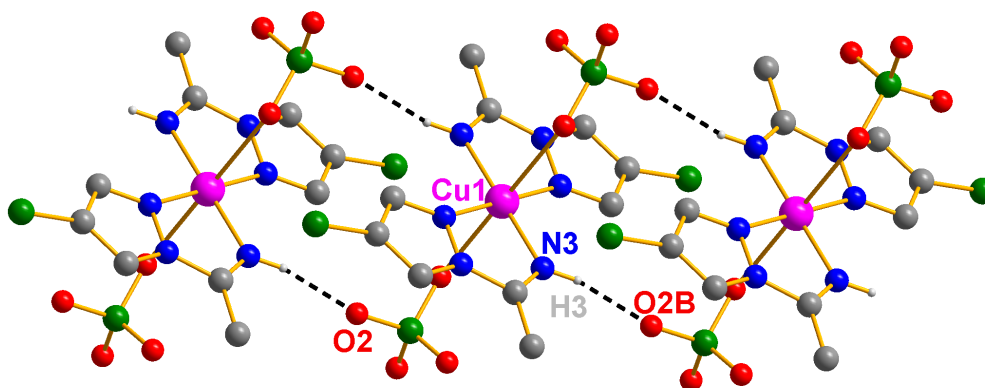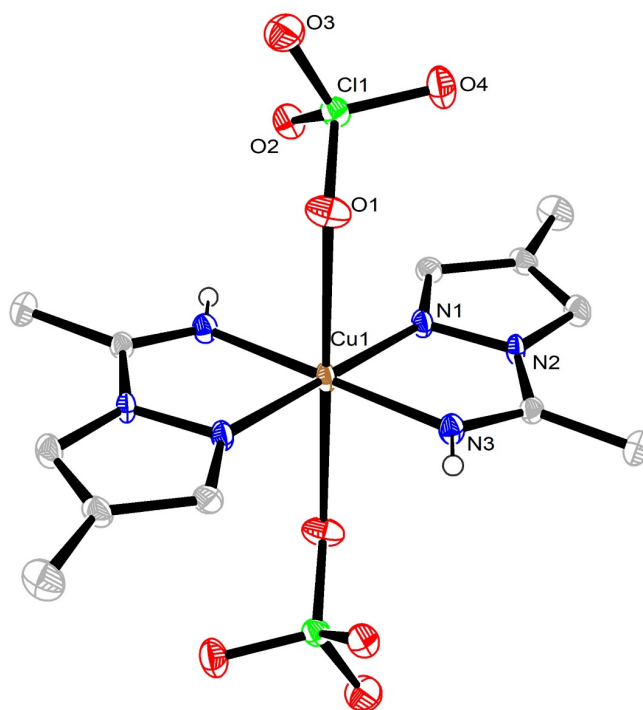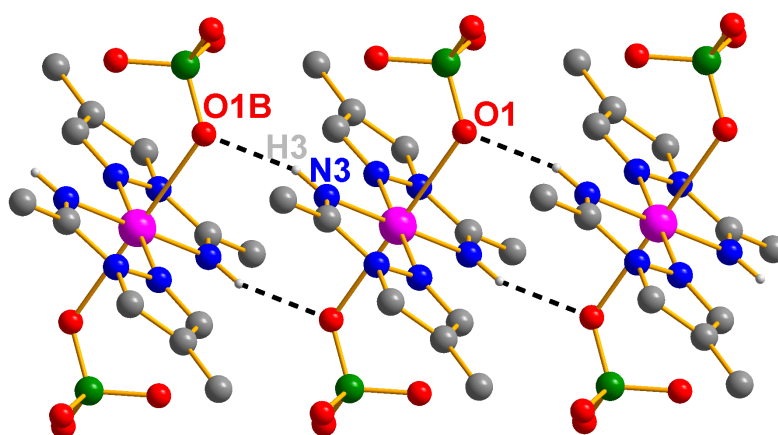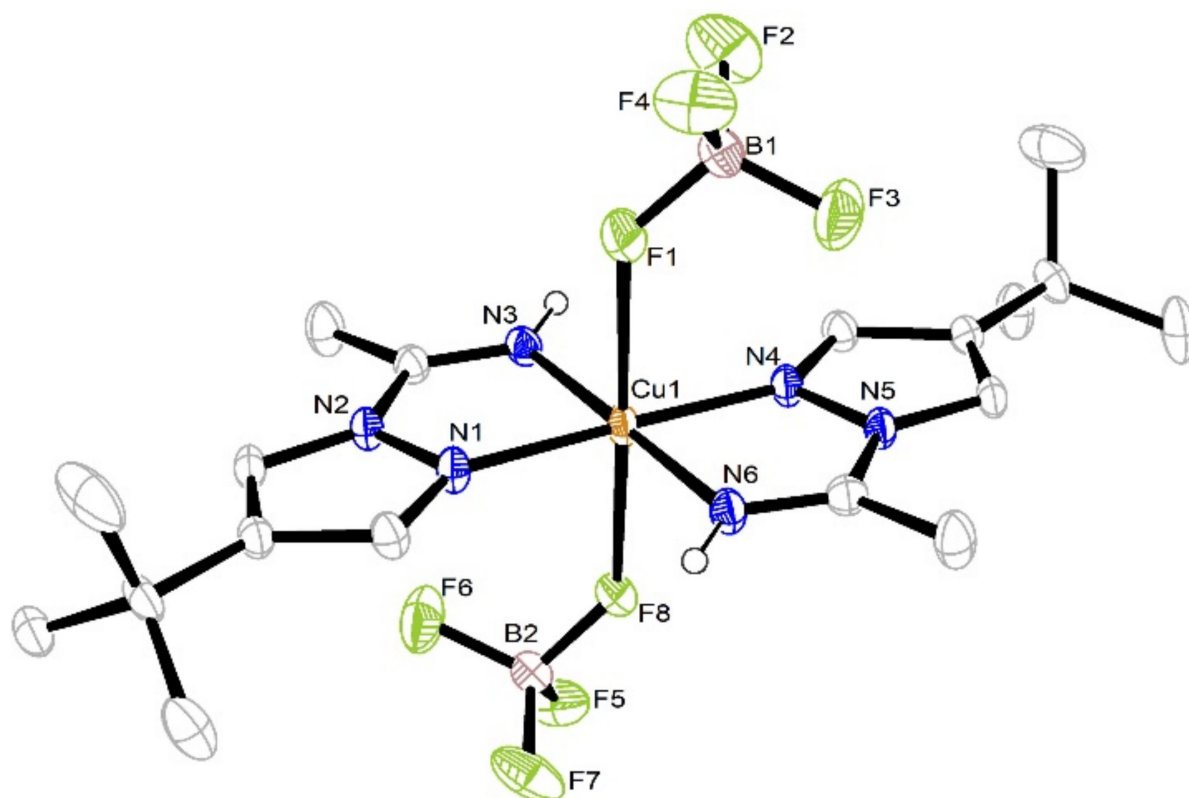
Figure S13. ORTEP style representation of **1e''**. Thermal ellipsoids are drawn at the 35% probability level. The hydrogen atoms bound to carbon atoms were omitted for clarity. Selected bond lengths [Å] and angles [°]: Cu1-N1 1.977(2), Cu1-N3 1.960(3), Cu1-N4 1.978(3), Cu1-N6 1.971(3), Cu1-F1 2.525(3), Cu1-F8 2.554(3), N1-Cu1-N3 80.64(12), N1-Cu1-N4 178.69(18), N1-Cu1-N6 98.91(12), N1-Cu1-F1 88.58(12), N1-Cu1-F8 91.33(11), N3-Cu1-N4 99.90(12), N3-Cu1-N6 179.47(14), N3-Cu1-F1 95.10(11), N3-Cu1-F8 82.03(11), N4-Cu1-N6 80.54(12), N4-Cu1-F1 92.56(11), N4-Cu1-F8 87.57(11), N6-Cu1-F1 85.17(11), N6-Cu1-F8 97.70(12), F1-Cu1-F8 177.10(11).
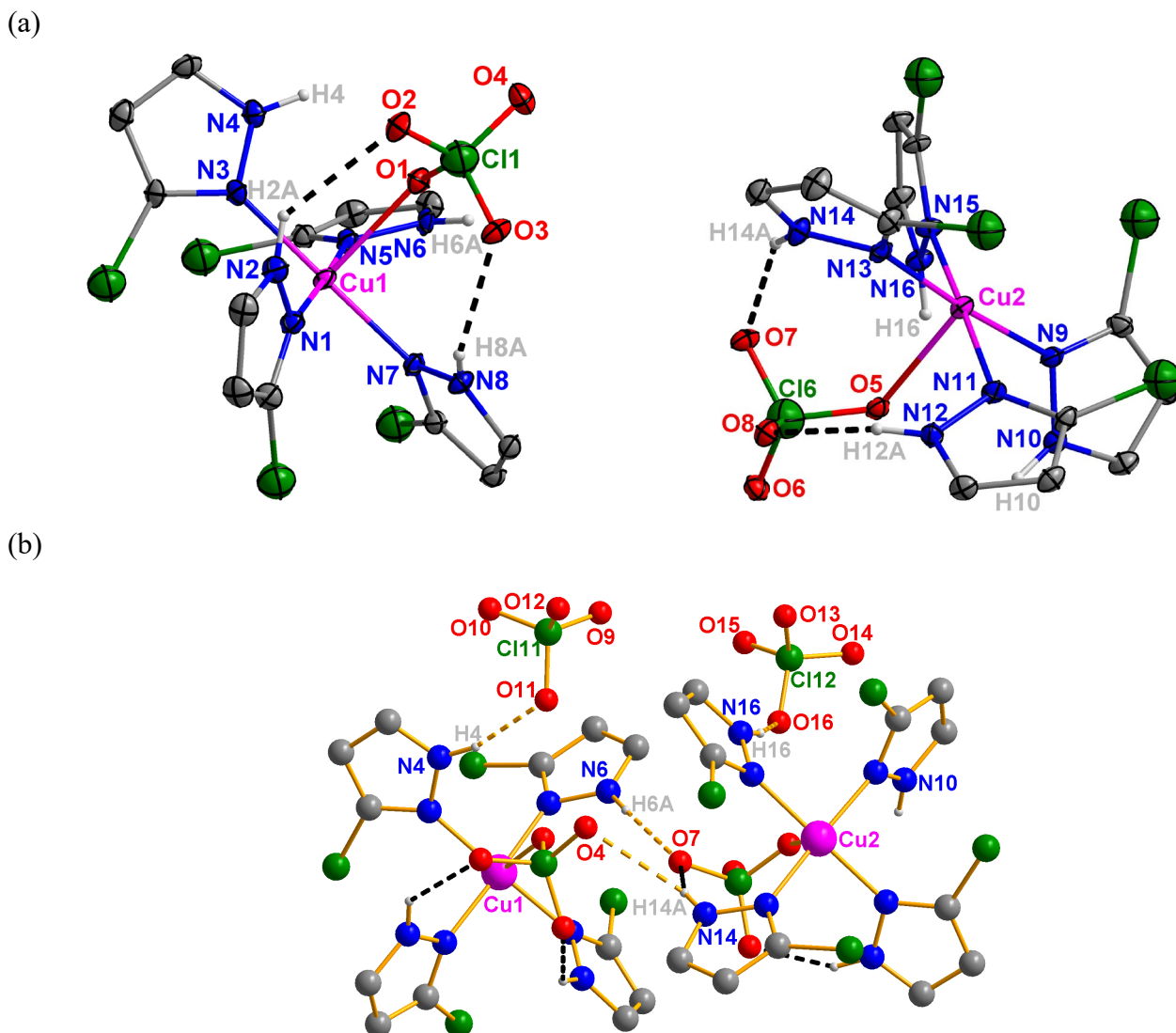
Figure S14-1. (a) ORTEP style representation of **2a** with the black dashed lines showing the intramolecular hydrogen-bond interactions. The structure has two independent molecules in the asymmetric unit cell. For each independent molecule (left and right), one unbound perchlorate counteranion is omitted for clarity and the thermal ellipsoids are drawn at the 35% probability level. (b) Ball-and-stick representation of **2a** with the yellow dashed lines showing the intermolecular hydrogen-bond interactions. The hydrogen atoms bound to carbon atoms were omitted for clarity. Selected bond lengths [Å] and angles [°]: Cu1-N1 2.007(5), Cu1-N3 2.013(5), Cu1-N5 1.985(5), Cu1-N7 2.020(5), Cu1-O1 2.285(5), N1-Cu1-N3 90.4(2), N1-Cu1-N5 174.7(2), N1-Cu1-N7 91.0(2), N1-Cu1-O1 101.2(2), N3-Cu1-N5 88.3(2), N3-Cu1-N7 178.6(2), N3-Cu1-O1 88.60(19), N5-Cu1-N7 90.4(2), N5-Cu1-O1 83.90(19), N7-Cu1-O1 91.08(19); Cu2-N9 1.994(5), Cu2-N11 2.006(5), Cu2-N13 2.004(5), Cu2-N15 1.996(5), Cu2-O5 2.303(4), N9-Cu2-N11 89.0(2), N9-Cu2-N13 174.4(2), N9-Cu2-N15 89.4(2), N9-Cu2-O5 82.83(18), N11-Cu2-N13 89.7(2), N11-Cu2-N15 177.1(2), N11-Cu2-O5 90.02(18), N13-Cu2-N15 92.1(2), N13-Cu2-O5 102.60(18), N15-Cu2-O5 87.36(18). H-bonding: N2···O2 3.068(8), H2···O2 2.368(5), N2-H2···O2 136.6(4); N8···O3 2.90(7), H8···O3 2.211(5), N8-H8···O3 136.1(4); N12···O8 3.027(7), H12···O8 2.231(5), N12-H12···O8 150.3(4); N14···O7 2.948(7), H14···O7 2.172(5), N14-H14···O7 146.9(4); N4···O11 2.840(8), H4···O11 1.984(5), N4-H4···O11 163.8(4); N6···O7 2.918(7), H6···O7 2.054(5), N6-H6···O7 167.1(4); N14···O4 3.156(7), H14···O4 2.568(5), N14-H14···O4 125.0(4); N16···O16 2.825(7), H16···O16 1.975(4), N16-H16···O16 162.0(3).

(a)
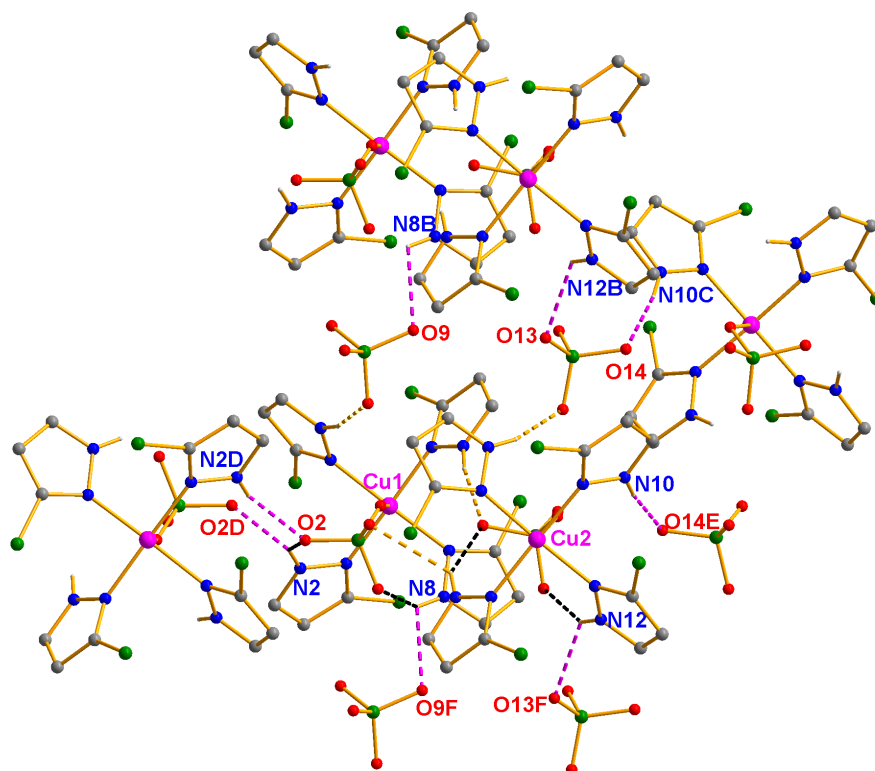
(b)
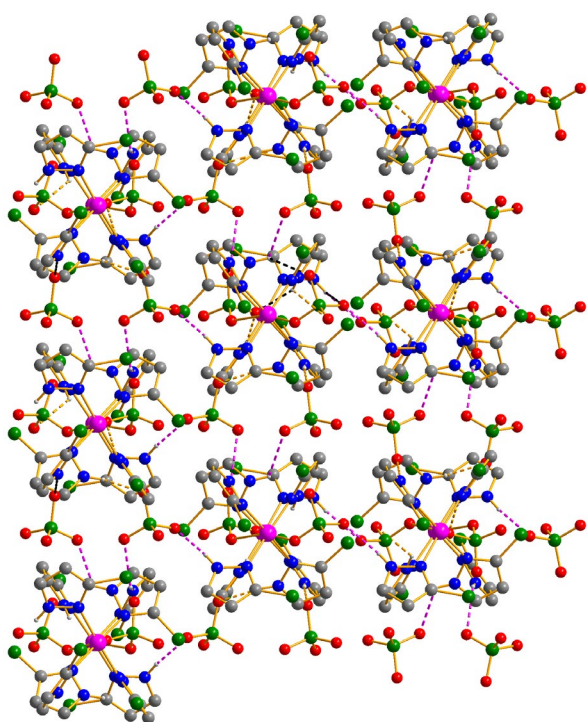
(c)
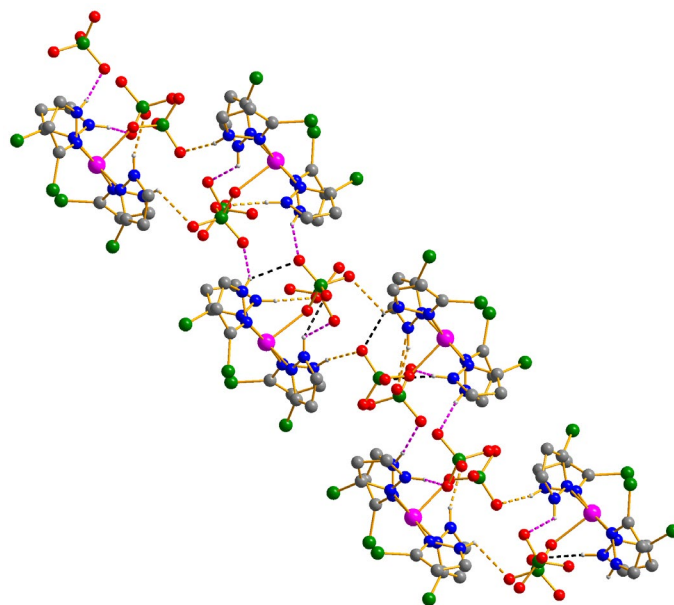
Figure S14-2. (a) Two-dimensional assembly of **2a** with the pink dashed lines showing the additional intermolecular hydrogen-bond interactions. Packing diagrams are depicted along the bc plane (b) and along the ac plane (c). Only the significant component is shown. The hydrogen atoms bound to carbon atoms were omitted for clarity. H-bonding: N2···O2D 2.881(8) Å, H2···O2D 2.094(5) Å, N2-H2···O2D 148.4(4)°; N8···O9F 3.047(8) Å, H8···O9F 2.550(5) Å, N8-H8···O9F 116.7(4)°; N10···O14E 2.870(7) Å, H10···O14E 1.997(5) Å, N10-H10···O14E 171.6(4)°; N12···O13F 2.986(7) Å, H12···O13F 2.388(5) Å, N12-H12···O13F 125.4(4)°. Symmetry code: D 1-x, 1-y, 1-z; E 3/2-x, 1/2+y, 3/2-z; F x, 1+y, z.

(a)
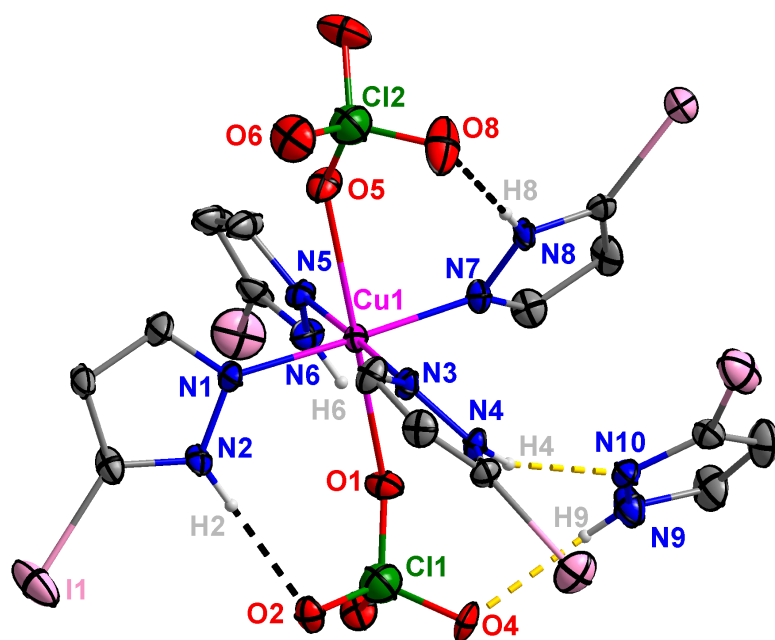
(b)

Figure S15. (a) ORTEP style representation of **2c** with the black and yellow dashed lines showing the intramolecular and intermolecular hydrogen-bond interactions, respectively. Thermal ellipsoids are drawn at the 35% probability level. The hydrogen atoms bound to carbon atoms were omitted for clarity. Selected bond lengths [Å] and angles [°]: Cu1-N1 2.018(7), Cu1-N3 1.995(7), Cu1-N5 2.004(7), Cu1-N7 1.990(7), Cu1-O1 2.560(6), Cu1-O5 2.502(7), N1-Cu1-N3 90.0(3), N1-Cu1-N5 88.1(3), N1-Cu1-N7 178.2(3), N1-Cu1-O1 93.6(2), N1-Cu1-O5 88.2(3), N3-Cu1-N5 178.0(3), N3-Cu1-N7 90.4(3), N3-Cu1-O1 95.3(3), N3-Cu1-O5 92.2(3), N5-Cu1-N7 91.5(3), N5-Cu1-O1 84.4(3), N5-Cu1-O5 88.3(3), N7-Cu1-O1 88.2(3), N5-Cu1-O5 90.0(3), O1-Cu1-O5 172.4(2). H-bonding: N2···O2 2.92(1), H2···O2 2.047(7), N2-H2···O2 173.1(5); N8···O8 2.85(1), H8···O8 1.995(9), N8-H8···O8 164.5(5); N9···O4 2.94(14), H9···O4 2.224(9), N9-H9···O4 137.9(6); N4···N10 2.88(1), H4···N10 2.056(8), N4-H4···N10 154.5(5). (b) One-dimensional packing diagram with the brown dashed lines showing the additional intermolecular NH···O hydrogen-bond interactions. Only the significant component is shown. H-bonding: N6···O6A 2.99(1) Å, H6···O6A 2.193(9) Å, N6-H6···O6A 151.2(6)°. Symmetry code: A 1+x, y, z.
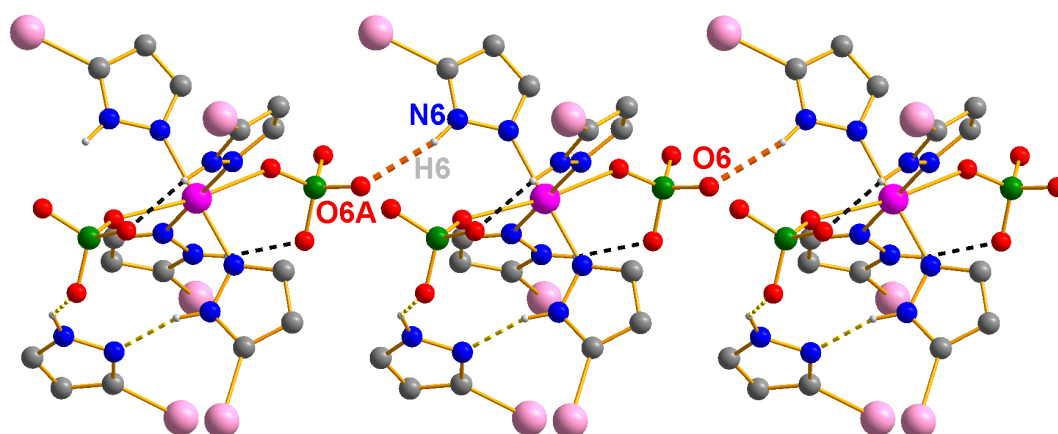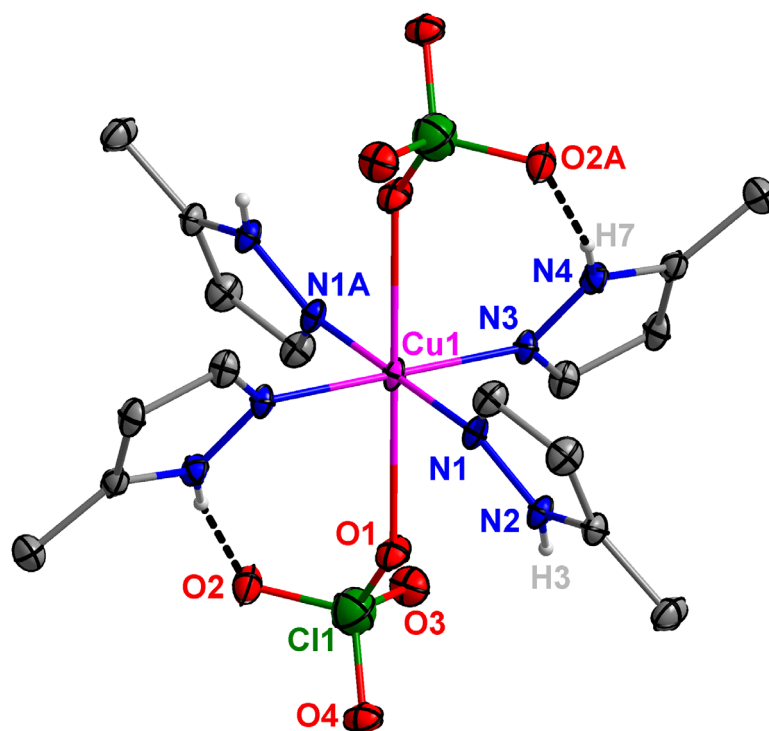
(a)

(b)

Figure S16. (a) ORTEP style representation of **2d** with the black dashed lines showing the intramolecular hydrogen-bond interactions. Thermal ellipsoids are drawn at the 35% probability level. The hydrogen atoms bound to carbon atoms were omitted for clarity. Selected bond lengths [Å] and angles [°]: Cu1-N1 2.002(2), Cu1-N3 1.997(2), Cu1-O1 2.4647(18), N1-Cu1-N3 88.08(9), N1-Cu1-O1 82.59(8), N1-Cu1-N1A 180.0, N1-Cu1-N3A 91.92(9), N1-Cu1-O1A 97.41(8), N3-Cu1-O1 91.70(8), N3-Cu1-N3A 180.0, N3-Cu1-O1A 88.30(8). H-bonding: N4···O2A 3.014(4), H7···O2A 2.144(3), N4-H7···O2A 169.1(2). Symmetry transformations used to generate equivalent atoms: A -x+1, -y+2, -z+1. (b) One-dimensional packing diagram with the black dashed lines showing the intermolecular NH···O hydrogen-bond interactions. Only the significant component is shown. H-bonding: N2···O4B 2.976(3) Å, H3···O4B 2.137(2) Å, N2-H3···O4B 159.3(2)°. Symmetry code: B 1-x, 1-y, 1-z.
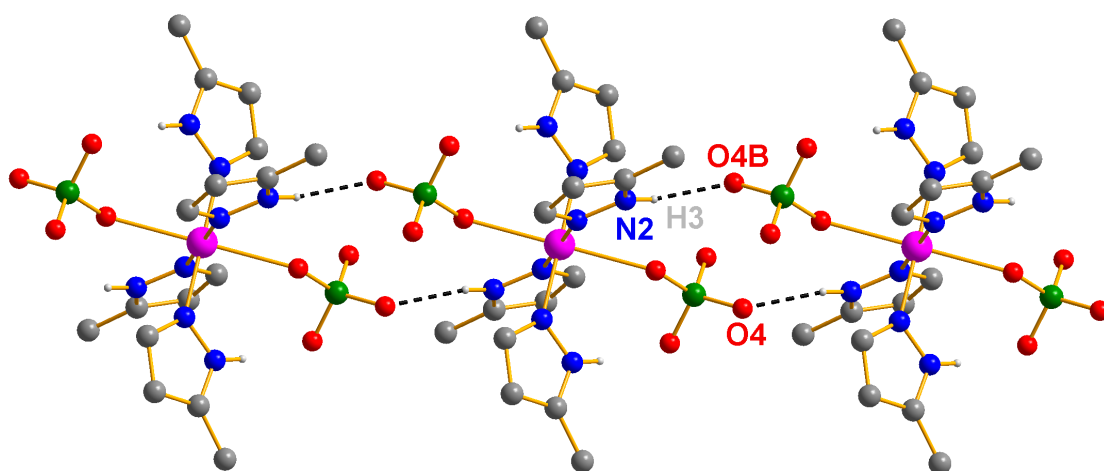
Figure S17. ORTEP style representation of **2e** with the black dashed lines showing the intramolecular hydrogen-bond interactions. Thermal ellipsoids are drawn at the 35% probability level. The hydrogen atoms bound to carbon atoms were omitted for clarity. Selected bond lengths [Å] and angles [°]: Cu1-N1 1.966(5), Cu1-N3 1.975(5), Cu1-N5 1.971(5), Cu1-N7 1.987(5), Cu1-O1 2.528(4), Cu1-O5 2.570(5), N1-Cu1-N3 88.71(19), N1-Cu1-N5 173.5(2), N1-Cu1-N7 92.07(19), N1-Cu1-O1 88.60(18), N1-Cu1-O5 104.55(18), N3-Cu1-N5 91.07(19), N3-Cu1-N7 170.1(2), N3-Cu1-O1 107.31(17), N3-Cu1-O5 87.20(18), N5-Cu1-N7 89.27(19), N5-Cu1-O1 85.22(18), N5-Cu1-O5 81.97(19), N7-Cu1-O1 82.55(17), N7-Cu1-O5 83.08(18), O1-Cu1-O5 160.83(15). H-bonding: N2···O2 2.930(6), H2···O2 2.10(4), N2-H2···O2 157.2(3); N4···O7 2.957(7), H4···O7 2.114(5), N4-H4···O7 160.3(3).
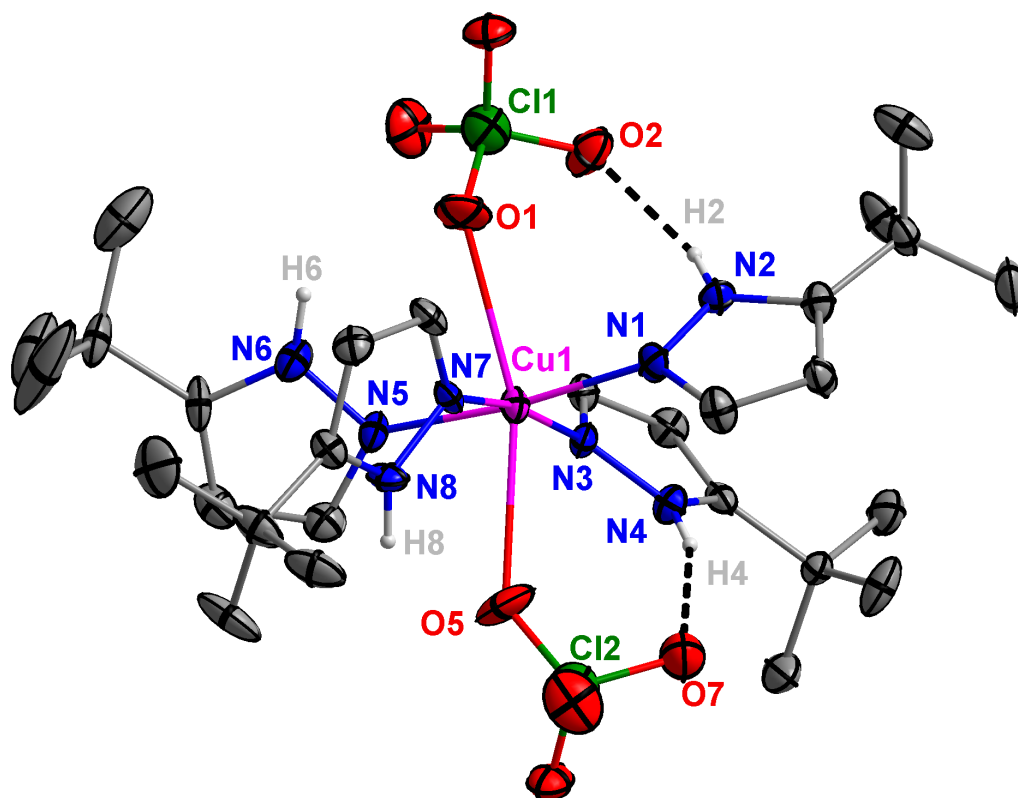
(a)

(b)

Figure S18. (a) ORTEP style representation of **2a'** with the black dashed lines showing the intramolecular hydrogen-bond interactions. Thermal ellipsoids are drawn at the 35% probability level. The hydrogen atoms bound to carbon atoms were omitted for clarity. Selected bond lengths [Å] and angles [°]: Cu1-N1 2.001(3), Cu1-N3 1.999(3), Cu1-O1 2.384(4), N1-Cu1-N3 179.17(16), N1-Cu1-O1 91.20(16), N1-Cu1-N1A 88.98(19), N1-Cu1-N3A 90.60(12), N1-Cu1-O1A 97.68(16), N3-Cu1-O1 88.15(16), N3-Cu1-N1A 90.60(12), N3-Cu1-N3A 89.81(19), N3-Cu1-O1A 83.04(16), O1-Cu1-O1A 167.56(17). H-bonding: N2···O3 3.040(5), H2···O3 2.253(4), N2-H2···O3 152.0(3). (b) Two-dimensional packing diagram with the yellow dashed lines showing the intermolecular NH···O hydrogen-bond interactions. Only the significant component is shown. H-bonding: N4···O3B 2.898(7) Å, H4···O3B 2.082(5) Å, N4-H4···O3B 158.2(3)°. Symmetry code: A 1-x, y, 1/2-z; B 3/2-x, 1/2+y, 1/2-z.
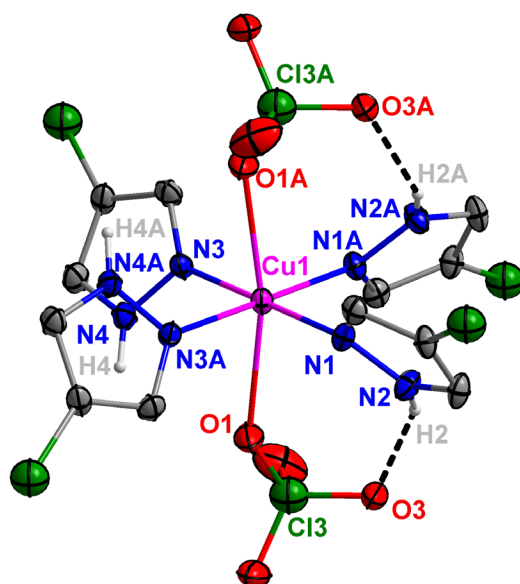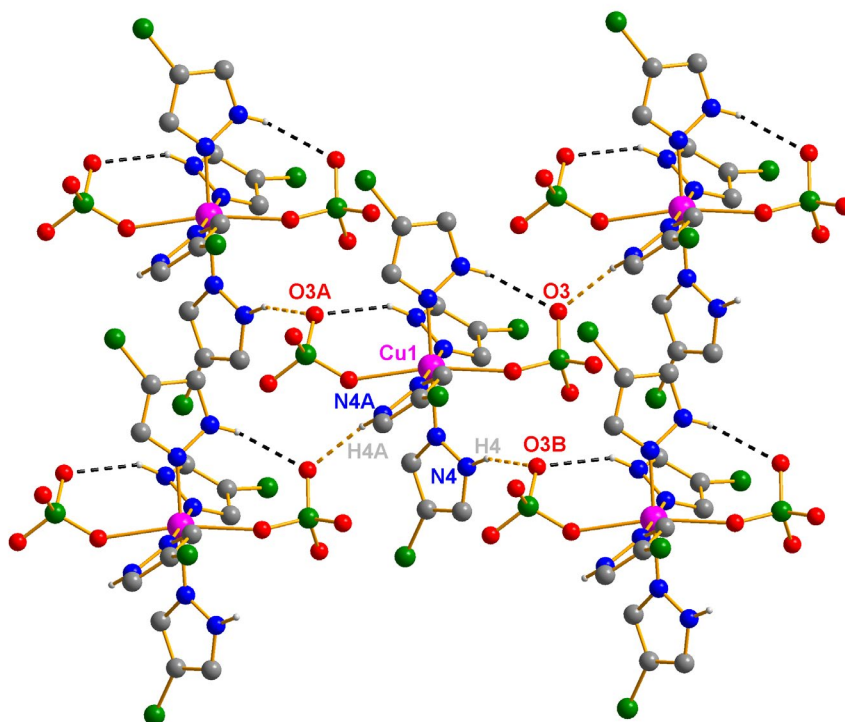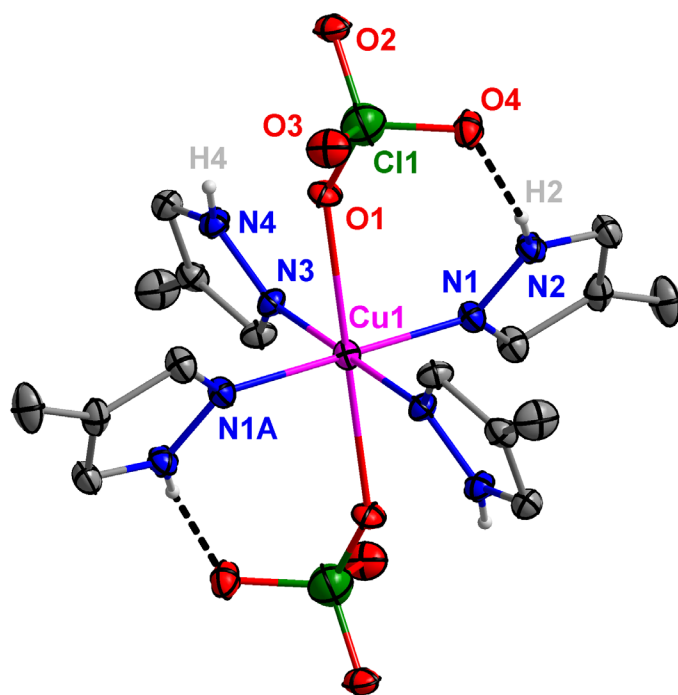
(a)

(b)

Figure S19. (a) ORTEP style representation of **2d'** with the black dashed lines showing the intramolecular hydrogen-bond interactions. Thermal ellipsoids are drawn at the 35% probability level. The hydrogen atoms bound to carbon atoms were omitted for clarity. Selected bond lengths [Å] and angles [°]: Cu1-N1 1.9993(14), Cu1-N3 2.0066(14), Cu1-O1 2.4411(11), N1-Cu1-N1A 180.0, N1-Cu1-N3 90.53(6), N1-Cu1-N3A 89.47(6), N1A-Cu1-N3, 89.47(6), N1A-Cu1-N3A 90.53(6), N3-Cu1-N3A 180.00(8), N1-Cu1-O1 92.88(5), N1A-Cu1-O1 87.12(5), N3-Cu1-O1 85.96(5), N3A-Cu1-O1 94.04(5). H-bonding: N2···O4 2.937(2), H2···O4 2.079(2), N2-H2···O4 164.7(1). Symmetry transformations used to generate equivalent atoms: A -x+2, -y+1, -z+1. (b) One-dimensional packing diagram with the black dashed lines showing the intermolecular NH···O hydrogen-bond interactions. Only the significant component is shown. H-bonding: N4···O2B 2.917(2) Å, H4···O2B 2.158(2) Å, N4-H4···O2B 144.1(1)°. Symmetry code: B 2-x, -y, 1-z.
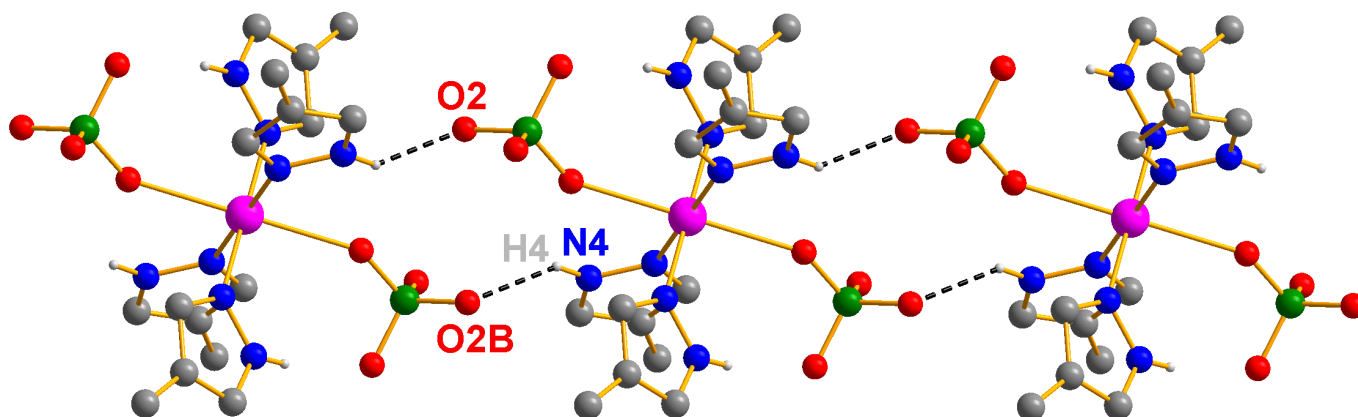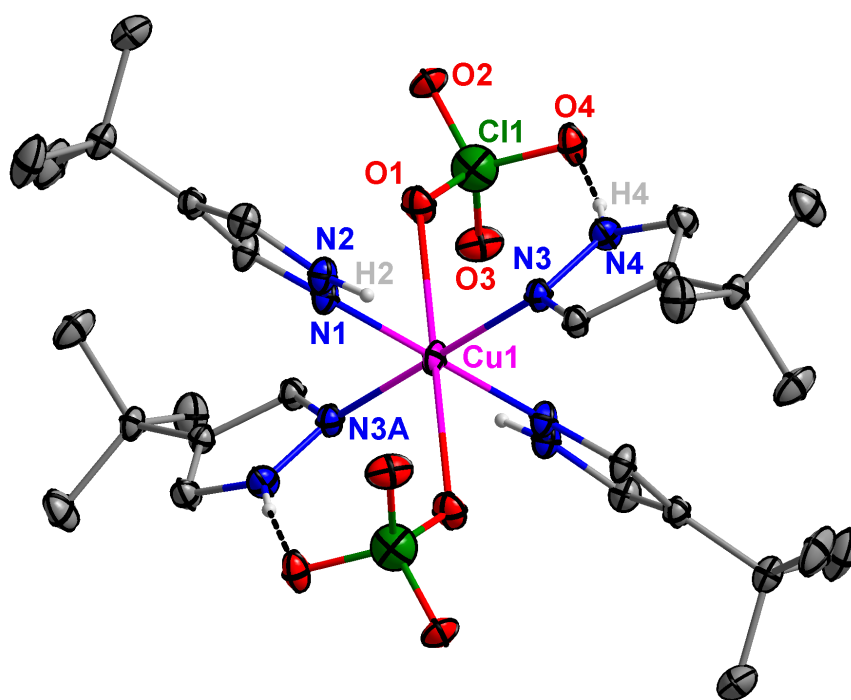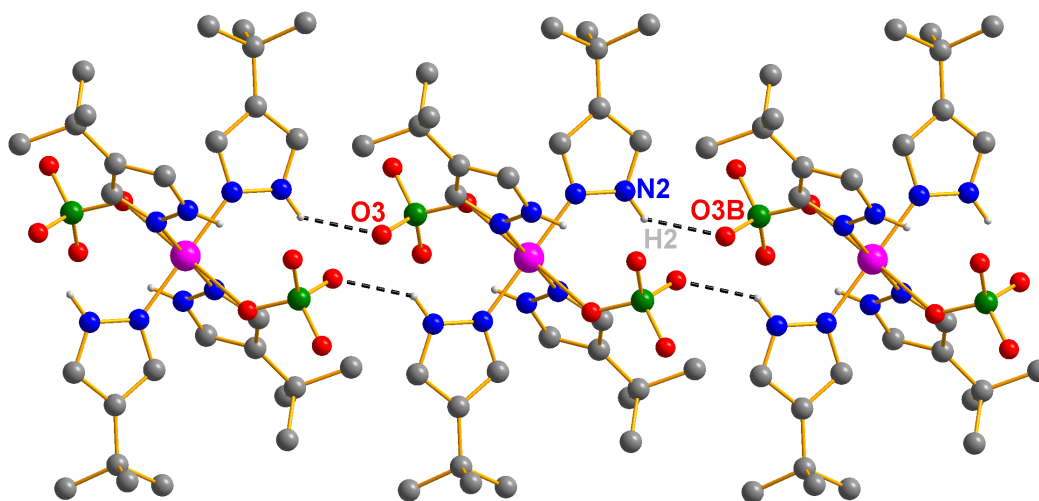
Figure S20. (a) ORTEP style representation of **2e'** with the black dashed lines showing the intramolecular hydrogen-bond interactions. Thermal ellipsoids are drawn at the 35% probability level. The hydrogen atoms bound to carbon atoms were omitted for clarity. Selected bond lengths [Å] and angles [°]: Cu1-N1 2.0048(13), Cu1-N1A 2.0048(13), Cu1-N3 2.0070(13), Cu1-N3A 2.0070(12), Cu1-O1 2.5033(11), N1-Cu1-N3 92.94(5), N1-Cu1-O1 82.96(5), N1-Cu1-N1A 180.0, N1-Cu1-N3A 87.06(5), N3-Cu1-O1 90.85(5), N3-Cu1-N1A 87.06(5), N3-Cu1-N3A 180.0, N3-Cu1-O1A 89.15(5), O1-Cu1-N1A 97.04(5), O1-Cu1-N3A 89.15(5). H-bonding: N4···O4 2.946(2), H4···O4 2.068(1), N4-H4···O4 174.7(1). Symmetry transformations used to generate equivalent atoms: A -x+1, -y+1, -z+1. (b) One-dimensional packing diagram with the black dashed lines showing the intermolecular NH···O hydrogen-bond interactions. Only the significant component is shown. H-bonding: N2···O3B 2.910(2) Å, H2···O3B 2.191(1) Å, N2-H2···O3B 138.7(1)°. Symmetry code: B 1+x, y, z.
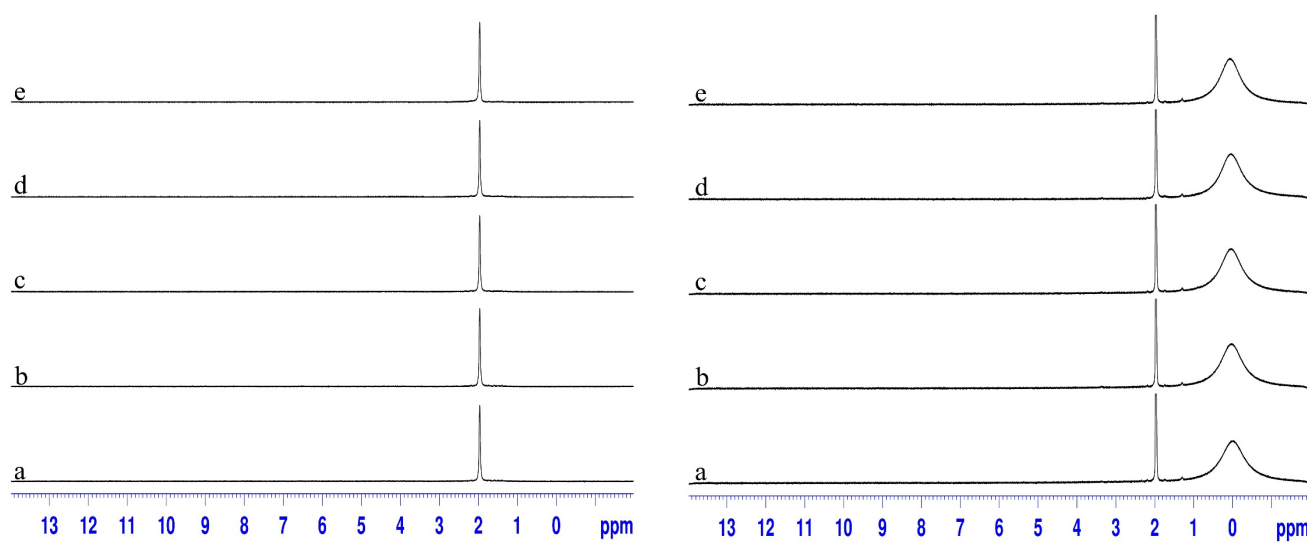
Figure S21. The time-dependent ^{1}H NMR spectra of **2a** (right) or **2d** (left) dissolved in *d*-MeCN at (a) 5 mins, (b) 15 mins, (c) 30 mins, (d) 45mins and (e) 60 mins.

Table S1. The optimized structures of predicted geometries and their energy differences for $[Cu(3(5)\text{-}ClPzH)_4]^{2+}$ with 2 ClO_4^-.
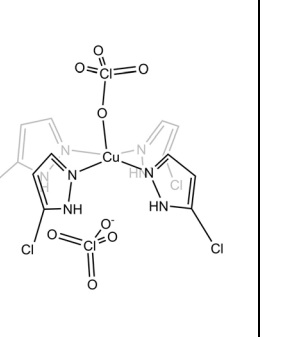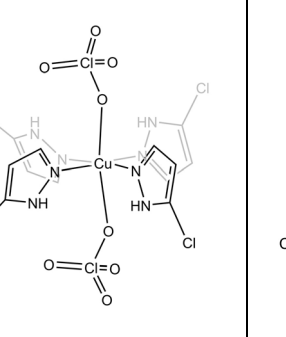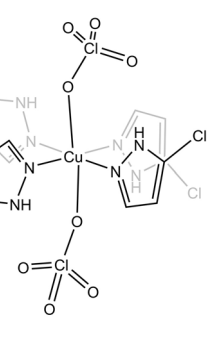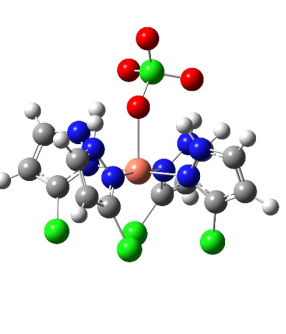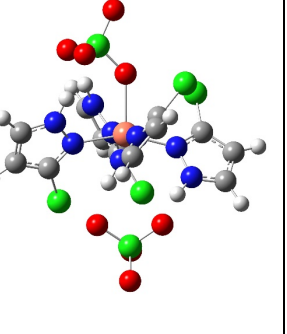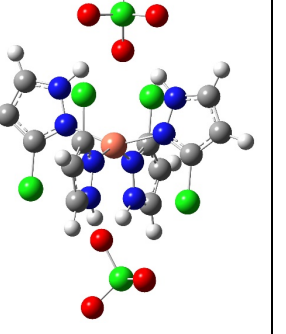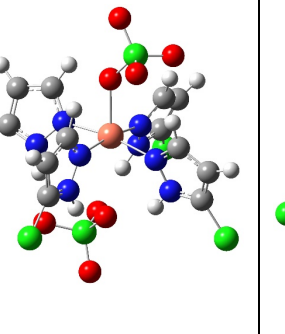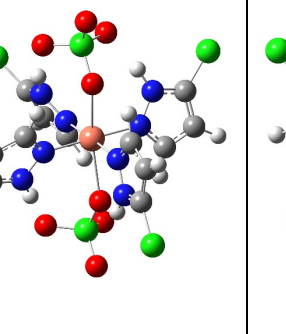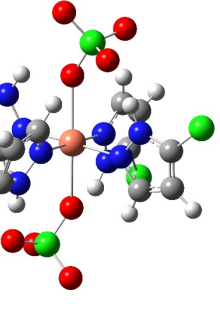
	[Cu(3-ClPzH)₄]²⁺			[Cu(5-ClPzH)₄]²⁺		
	2a					
ΔKcal/mol	97.86077436	11.68453113	12.23289329	4.078783625	0	1.633609333

Table S2. The optimized structures of predicted geometries and their energy differences for [Cu(3(5)-MePzH)$_4$]$^{2+}$ with 2 ClO$_4^-$.

	[Cu(3-MePzH)$_4$]$^{2+}$			[Cu(5-MePzH)$_4$]$^{2+}$		
					2d	
ΔKcal/mol	99.66118213	8.653344075	11.1180904	2.613202644	0	0.517149816

Table S3. The summary of crystallographic data for the complexes.

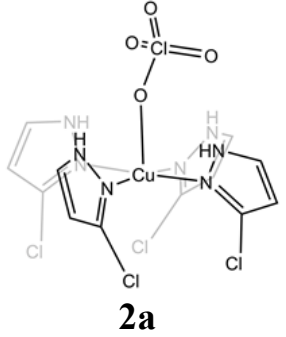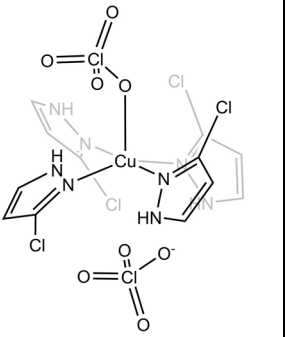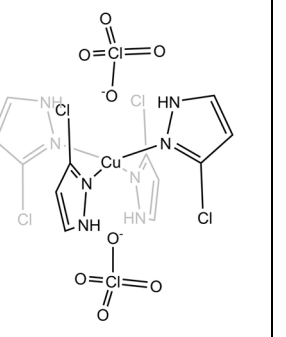|	1a	1b	1c	1d	1a'
formula	C10 H12 Cl4 Cu N6 O8	C10 H12 Br2 Cl2 Cu N6 O8	C10 H12 Cl2 Cu I2 N6 O8	C12 H18 Cl2 Cu N6 O8	C10 H12 Cl4 Cu N6 O8
fw	549.61	638.51	732.51	508.76	549.61
temp, K	150(2)	150(2)	150(2)	150(2)	150(2)
cryst syst	Triclinic	Monoclinic	Monoclinic	Monoclinic	Triclinic
space group	P-1	P21/n	P21/c	P21/n	P-1
a, Å	7.0595(2)	7.8326(4)	7.9186(3)	7.8033(5)	6.5992(3)
b, Å	7.7575(2)	10.9412(7)	11.1291(3)	9.4838(6)	8.3622(4)
c, Å	9.7194(3)	11.5905(7)	13.1374(4)	12.8328(8)	9.3885(5)
α, °	81.015(2)	90	90	90	81.900(3)
β, °	84.024(2)	97.897(2)	117.5270(10)	107.447(4)	74.576(3)
γ, °	68.617(2)	90	90	90	74.932(3)
Volume, Å^3 / Z	488.91(3) / 1	983.86(10) / 2	1026.69(6) / 2	906.00(10) / 2	480.83(4) / 1
Density (cald.), Mg/m^3	1.867	2.155	2.369	1.865	1.898
Absorption coefficient, mm^{-1}	1.716	5.496	4.382	1.559	1.745
crystal size, mm	0.120 x 0.080 x 0.020	0.28 x 0.10 x 0.08	0.18 x 0.11 x 0.09	0.120 x 0.060 x 0.040	0.18 x 0.02 x 0.02
θ range, deg	2.124 to 28.705	2.572 to 28.952°	2.531 to 28.753	2.717 to 28.743	2.257 to 28.760
no. of reflns collected	7716	13025	15311	29538	6162
no. of indep reflns	2501	2559	2654	2352	2450
max. and min. trans	0.837 and 0.404	0.644 and 0.522	0.616 and 0.496	0.940 and 0.835	0.930 and 0.916
no. of data /restraints /params	2501 / 0 / 134	2559 / 0 / 134	2654 / 0 / 134	2352 / 0 / 135	2450 / 0 / 134
goodness-of-fit on F^2	0.880	1.239	1.272	1.019	1.021
final R indices [$I>2\sigma(I)$] $R_1{}^a$, $wR_2{}^b$	0.0319, 0.1073	0.0439, 0.0829	0.0449, 0.0646	0.0368, 0.1299	0.0345, 0.0857
R indices (all data), $R_1{}^a$,$wR_2{}^b$	0.0375, 0.1151	0.0535, 0.0848	0.0712, 0.0681	0.0475, 0.1512	0.0402, 0.0898
largest diff. peak and hole, e Å^{-3}	0.827 and -0.567	0.811 and -1.244	1.381 and -1.309	0.618 and -0.380	0.611 and -0.469

[a] $R_1 = \Sigma \left| F_0 \right| - \left| F_c \right| / \Sigma \left| F_0 \right|$ [b] $wR_2 = [\Sigma[\omega(F_0{}^2 - F_c{}^2)^2] / \Sigma[\omega(F_0{}^2)^2]^{1/2}$

	1d'	1e"	2a	2c	2d
formula	C12 H18 Cl2 Cu N6 O8	C18 H30 B2 Cu F8 N6	C12 H12 Cl6 Cu N8 O8+[solvent]	C15 H15 Cl2 Cu I5 N10 O8	C16 H24 Cl2 Cu N8 O8
fw	508.77	567.64	672.55	1232.32	590.88
temp, K	150(2)	150(2) K	150.04(10)	150(2)	150(2)
cryst syst	Monoclinic	Orthorhombic	Monoclinic	Monoclinic	Triclinic
space group	P21/n	Pca2$_1$	C2/c	Cc	P-1
a, Å	5.3447(3)	31.3023(4)	31.7856(3)	8.9446(7)	8.8912(5)
b, Å	13.7312(7)	7.10072(7)	9.81790(10)	23.069(2)	8.8939(6)
c, Å	13.2253(6)	11.71542(15)	31.0513(3)	15.8266(11)	9.1265(6)
α, °	90	90	90	90	90.491(4)
β, °	92.850(4)	90	97.6950	94.659(3)	117.756(4)
γ, °	90	90	90	90	110.978(4)
Volume, Å3 / Z	969.39(9) / 2	2603.97(5) / 4	9602.85(16) / 16	3255.0(5) / 4	582.75(7) / 1
Density (cald.), Mg/m3	1.743	1.448	1.861	2.515	1.684
Absorption coefficient, mm-1	1.457	1.876	7.966	5.631	1.227
crystal size, mm	0.120 x 0.040 x 0.040	0.220 x 0.050 x 0.050	0.12 x 0.08 x 0.03	0.360 x 0.260 x 0.150	0.120 x 0.080 x 0.040
θ range, deg	2.139 to 28.741	2.823 to 74.841	2.806 to 74.912	2.854 to 27.896	2.581 to 28.282°.
no. of reflns collected	13785	17905	9641	70701	10047
no. of indep reflns	2510	4862	9641	7621	2880
max. and min. trans	0.906 and 0.751	1.00000 and 0.91336	1.00000 and 0.48482	0.237 and 0.085	0.920 and 0.784
no. of data /restraints /params	2510 / 0 / 135	4862 / 1 / 325	9641 / 0 / 632	7621 / 2 / 371	2880 / 0 / 162
goodness-of-fit on F2	0.993	1.056	1.072	0.918	0.892
final R indices [I>2σ(I)] R1a, wR2b	0.0441, 0.1333	0.0325, 0.0822	0.0760, 0.3696	0.0312, 0.1011	0.0418, 0.1186
R indices (all data), R1a ,wR2b	0.0596, 0.1445	0.0351, 0.0842	0.0807, 0.3770	0.0339, 0.1044	0.0535, 0.1299
largest diff. peak and hole, e Å-3	0.595 and -0.806	0.254 and -0.301	2.205 and -1.137	2.472 and -0.948	0.984 and -1.182

[a] $R_1 = \Sigma \left| F_0 \right| - \left| F_c \right| / \Sigma \left| F_0 \right|$ [b] $wR_2 = [\Sigma[\omega(F_0{}^2 - F_c{}^2)^2] / \Sigma[\omega(F_0{}^2)^2]^{1/2}$

	2e	2a'	2d'	2e'
formula	C28 H48 Cl2 Cu N8 O8	C12 H12 Cl6 Cu N8 O8	C16 H24 Cl2 Cu N8 O8	C28 H48 Cl2 Cu N8 O8
fw	759.19	672.55	590.87	759.18
temp, K	150(2)	150(2)	150(2)	150(2) K
cryst syst	Monoclinic	Monoclinic	Triclinic	Triclinic
space group	$P2_1/c$	C2/c	P-1	P-1
a, Å	11.8424(9)	13.4839(7)	8.6343(3)	8.7271(2)
b, Å	23.1795(19)	10.0715(4)	8.8087(3)	9.8586(2)
c, Å	13.7638(12)	19.0127(11)	9.9056(3)	12.2365(3)
α, °	90	90	65.897(3)	77.454(2)
β, °	94.605(7)	110.77	88.662(2)	85.620(2)
γ, °	90	90	63.858(3)	64.130(2)
Volume, Å3 / Z	3766.0(5) / 4	2414.2(2 / 4)	605.98(4) / 1	924.47(4) / 1
Density (cald.), Mg/m3	1.339	1.850	1.619	1.364
Absorption coefficient, mm-1	0.776	1.625	3.832	2.630
crystal size, mm	0.650 x 0.040 x 0.040	0.14 x 0.06 x 0.04	0.140 x 0.100 x 0.060	0.110 x 0.070 x 0.030
θ range, deg	1.725 to 25.048	2.291 to 28.876	4.983 to 74.320	3.701 to 74.823
no. of reflns collected	6636	3166	7079	10851
no. of indep reflns	6636	3166	2325	3567
max. and min. trans	0.959 and 0.549	0.940 and 0.890	1.00000 and 0.86499	3567 / 0 / 221
no. of data /restraints /params	6636 / 1 / 437	3166 / 0 / 160	2325 / 0 / 163	3567 / 0 / 221
goodness-of-fit on F2	0.812	0.982	0.992	1.033
final R indices [I>2σ(I)] R1a, wR2b	0.0634, 0.1380	0.0601, 0.1365	0.0251, 0.0719	0.0276, 0.0740
R indices (all data), R1a ,wR2b	0.1447, 0.1643	0.0712, 0.1455	0.0256, 0.0724	0.0288, 0.0747
largest diff. peak and hole, e Å-3	0.864 and -0.820	2.242 and -1.005	0.246 and -0.307	0.328 and -0.342

[a] $R_1 = \Sigma \left| F_0 \right| - \left| F_c \right| / \Sigma \left| F_0 \right|$ [b] $wR_2 = [\Sigma[\omega(F_0^2 - F_c^2)^2] / \Sigma[\omega(F_0^2)^2]^{1/2}$